Bioorganic & Medicinal Chemistry 17 (2009) 7021–7030

Contents lists available at ScienceDirect

Bioorganic & Medicinal Chemistry

journal homepage: www.elsevier.com/locate/bmc

Identification of small molecule regulators of the nuclear receptor HNF4α based on naphthofuran scaffolds

Rémy Le Guével [a,†,‡], Frédérik Oger [a,‡], Aurélien Lecorgne [b], Zuzana Dudasova [c], Soizic Chevance [b], Arnaud Bondon [d], Peter Barath [c], Gérard Simonneaux [b], Gilles Salbert [a,*]

[a] Equipe SPARTE, Université de Rennes 1, UMR6026 CNRS, Campus de Beaulieu, Bat 13, 35042 Rennes Cedex, France
[b] Equipe ICMV, Université de Rennes 1, UMR6226 CNRS, Campus de Beaulieu, Bat 10C, 35042 Rennes Cedex, France
[c] Cancer Research Institute, Slovak Academy of Sciences, Vlarska 7, SK-833 91 Bratislava, Slovak Republic
[d] Equipe RMN-ILP, Université de Rennes 1, UMR6026 CNRS, Campus de Beaulieu, Bat 13, 35042 Rennes Cedex, France

ARTICLE INFO

Article history:
Received 12 May 2009
Revised 24 July 2009
Accepted 26 July 2009
Available online 5 August 2009

Keywords:
Nuclear receptors
HNF4
Naphthofuran
Yeast one-hybrid system
Linoleic acid

ABSTRACT

Nuclear receptors are ligand-activated transcription factors involved in all major physiological functions of complex organisms. In this respect, they are often described as drugable targets for a number of pathological states including hypercholesterolemia and atherosclerosis. HNF4α (NR2A1) is a recently 'deorphanized' nuclear receptor which is bound in vivo by linoleic acid, although this natural ligand does not seem to promote transcriptional activation. In mouse, HNF4α is a major regulator of liver development and hepatic lipid metabolism and mutations in human have been linked to diabetes. Here, we have used a yeast one-hybrid system to identify small molecule activators of HNF4α in a library of synthetic compounds and found one hit bearing a methoxy group branched on a nitronaphthofuran backbone. A collection of molecules deriving from the discovered hit was generated and tested for activity toward HNF4α in yeast one-hybrid system. It was found that both the nitro group and a complete naphthofuran backbone were required for full activity of the compounds. Furthermore, adding a hydroxy group at position 7 of the minimal backbone led to the most active compound of the collection. Accordingly, a direct interaction of the hydroxylated compound with the ligand binding domain of HNF4α was detected by NMR and thermal denaturation assays. When used in mammalian cell culture systems, these compounds proved to be highly toxic, except when methylated on the furan ring. One such compound was able to modulate HNF4α-driven transcription in transfected HepG2C3A cells. These data indicate that HNF4α activity can be modulated by small molecules and suggest new routes for targeting the receptor in humans.

1. Introduction

Orphan nuclear receptors are members of the nuclear receptor superfamily of ligand regulated transcription factors for which ligands have not been identified.[1] Hepatocyte Nuclear Factor-4α, also known as HNF4α, is a highly conserved member of this nuclear receptor family that is expressed in liver, kidney, intestine, and pancreas, activates transcription likely as a homodimer[2] and was considered as an orphan receptor until very recently. In the liver, HNF4α is known to up-regulate transcription of the cholesterol 7α-hydroxylase (*Cyp7a1*) gene encoding a major cholesterol catabolizing enzyme and is itself targeted by bile acids in a complex feed-back regulatory loop.[3,4] Thus, HNF4α is an attractive target for the design and development of a new generation of hypolidemic agents.[5] Although fatty acyl-coenzyme A thioesters have been proposed to modulate HNF4α activity,[6] it has been reported later[7] that these molecules are not good candidates for being classical ligands for HNF4α. Fatty acids have also been suggested as endogeneous ligands of HNF4α on a structural basis. Indeed, they were found in the ligand binding pockets of crystallized HNF4α and HNF4γ.[8,9] However the crystallized HNF4α ligand binding domain (LBD) dimer is not in the fully active conformation since one monomer has helix 12 extended instead of the canonical 'closed' conformation observed in all activated receptors.[10] Fatty acid fitting into a nuclear receptor ligand binding pocket is a recurrent observation that has been made for several other LBDs expressed in *Escherichia coli* and crystallized (ERα, RXRα, RORβ, PPARβ/δ). What is unusual however, in the case of HNF4α and γ LBDs produced in *E. coli*, is that the bound fatty acid cannot be exchanged.[9,11] These data suggested that fatty acids may be structural determinants of HNF4α rather than ligands regulating conformational transitions. A recent study highlighted linoleic acid as an endogenous HNF4α ligand in cultured mammalian cells as well as

* Corresponding author. Tel.: +33 223 23 66 25; fax: +33 223 23 67 94.
E-mail address: gilles.salbert@univ-rennes1.fr (G. Salbert).
† Present address: U522 INSERM, Faculté de Médecine, Campus de Villejean, 35033 Rennes, France.
‡ These two authors contributed equally to this study.

0968-0896/$ - see front matter © 2009 Elsevier Ltd. All rights reserved.
doi:10.1016/j.bmc.2009.07.079

in mouse liver, but no function in the regulation of HNF4α transcriptional activity could be attributed to the newly discovered ligand.[12] Interestingly, linoleic acid can be exchanged from the receptor ligand binding pocket in cells.[12] Furthermore, in fasted animals, the ligand binding pocket was found to be devoid of ligand, indicating that, in certain physiological situations, HNF4α exists in the apo form. Hence, synthetic or natural molecules other than fatty acids might be used to manipulate HNF4α activity. If such synthetic compounds were to be obtained, they would prove to be extremely useful in precisely defining the physiological functions of HNF4α and would provide tools to intervene in physiological disorders like hypercholesterolemia.

In an attempt to identify HNF4α agonists, the initial screening of the National Center Institute (NCI, USA) diversity set of synthetic compounds (1990 molecules) was first undertaken in a yeast one-hybrid system. We discovered 4-methoxy-2-nitronaphtho[2,1-*b*]furan (**1**, Table 1) that modulates HNF4α activity in yeast, at the micromolar range. Through similarity searching of the complete library (250,000 compounds), we generated a first focused library containing 5 additional compounds (**2–6**) (Table 1) which were able to stimulate HNF4α-mediated transcription, compound **2** leading to the highest level of transcriptional induction. Synthesis of these molecules, were previously described by Royer and Buisson.[13] Because we found that these compounds also appeared to reduce yeast growth, we chose to prepare a series of related derivatives and analogs for further investigation. Since substitution in position 7 seemed to give the most active compound such as 7-methoxy-2-nitronaphtho[2,1-*b*]furan (**2**), we decided to set up a new series with aromatic ring linked in this position. Thus, the application of a Suzuki–Miyaura cross-coupling approach[14] to a range of phenyl C-7 substituted 2-nitronaphtho[2,1-*b*]furan from a 7-bromo-2-nitronaphtho[2,1-*b*]furan (**21a**) was undertaken.

Here, we report the identification of new activators of HNF4α using a random screening method through a yeast cell-based functional approach. We also report the chemical optimization study of the initial hit which led to the identification of a series of compounds that exhibit HNF4α agonist activities.

2. Chemistry

The strategy for hit modification is summarized in Scheme 1. To complete the series, starting from 2-nitronaphtho[2,1-*b*]furan, all the proposed synthetic modifications classified in two series are summarized in Tables 2–4. The compound 7-methoxy-2-nitronaphtho[2,1-*b*]furan (**2**) was chosen as starting material and different modifications of this compound have been made such as the substitution (or modification) of methoxy group in position 7 or the substitution of nitro group in position 2 (Table 2).

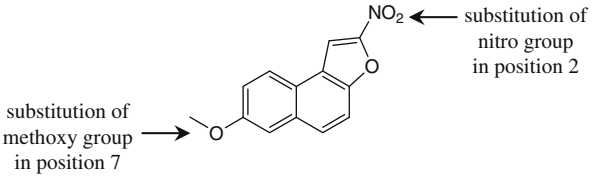

Scheme 1.

We have also prepared 2-nitronaphtho[2,3-*b*]furan (**18**), (*E*)-6-methoxy-1-(2-nitrovinyl)naphthalen-2-ol (**19**), and 6-methoxy-1-(2-nitroethyl)naphthalen-2-ol (**20**) (Table 3). Finally, we have also decided to explore Suzuki–Miyaura cross-coupling reaction starting from 7-bromo-2-nitronaphtho[2,1-*b*]furan (**21a**) to increase the hydrophobicity of the compounds (Table 4).

We started with the classical preparation of 2-nitronaphtho[2,1-*b*]furan derivatives. The first general method for synthesizing 2-nitrobenzo[*b*]furans of biological interest was the condensation between 2-hydroxybenzaldehyde and bromonitromethane reported by Royer et al.[15] Since then, this method was improved[16] and extended to the 2-nitronaphthofuran series[17] by the same group. Therefore, a first synthetic route for the construction of 2-nitronaphtho[2,1-*b*]furan ring was adapted from this

Table 1
Active compounds found from similarity search

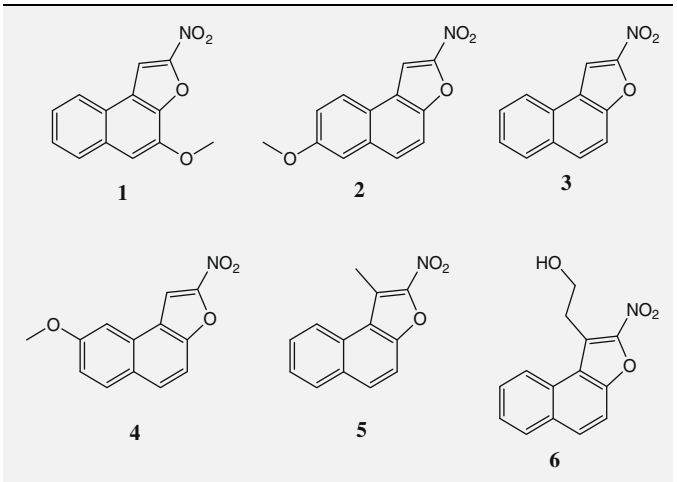

Table 2
First series of synthetic 2-nitronaphtho[2,1-*b*]furan and related derivatives (modifications in position 2 and in position 7)

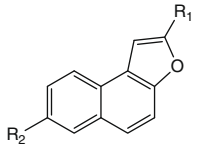

Compounds	R_1	R_2	Reference
2	NO_2	OCH_3	21
3	NO_2	H	17
7	NO_2	OH	19
8	NO_2	OCH_2COOEt	17
9	NO_2	OCH_2COOH	17
10	COOEt	H	18
11	COOEt	OCH_3	18
12	COOH	H	18
13	COOH	OCH_3	18
14	$CONH_2$	H	New
15	COOH	OCH_2COOH	New
16	H	OMe	20
17	H	H	20

Table 3
Other synthetic compounds tested on HNF4

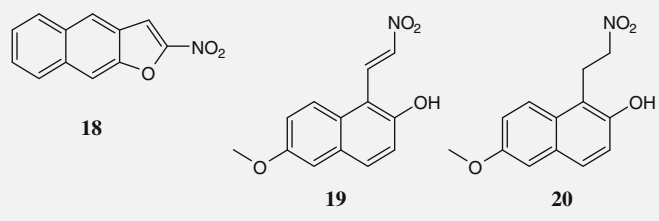

Table 4
Compound synthesized using Suzuki–Miyaura coupling reaction

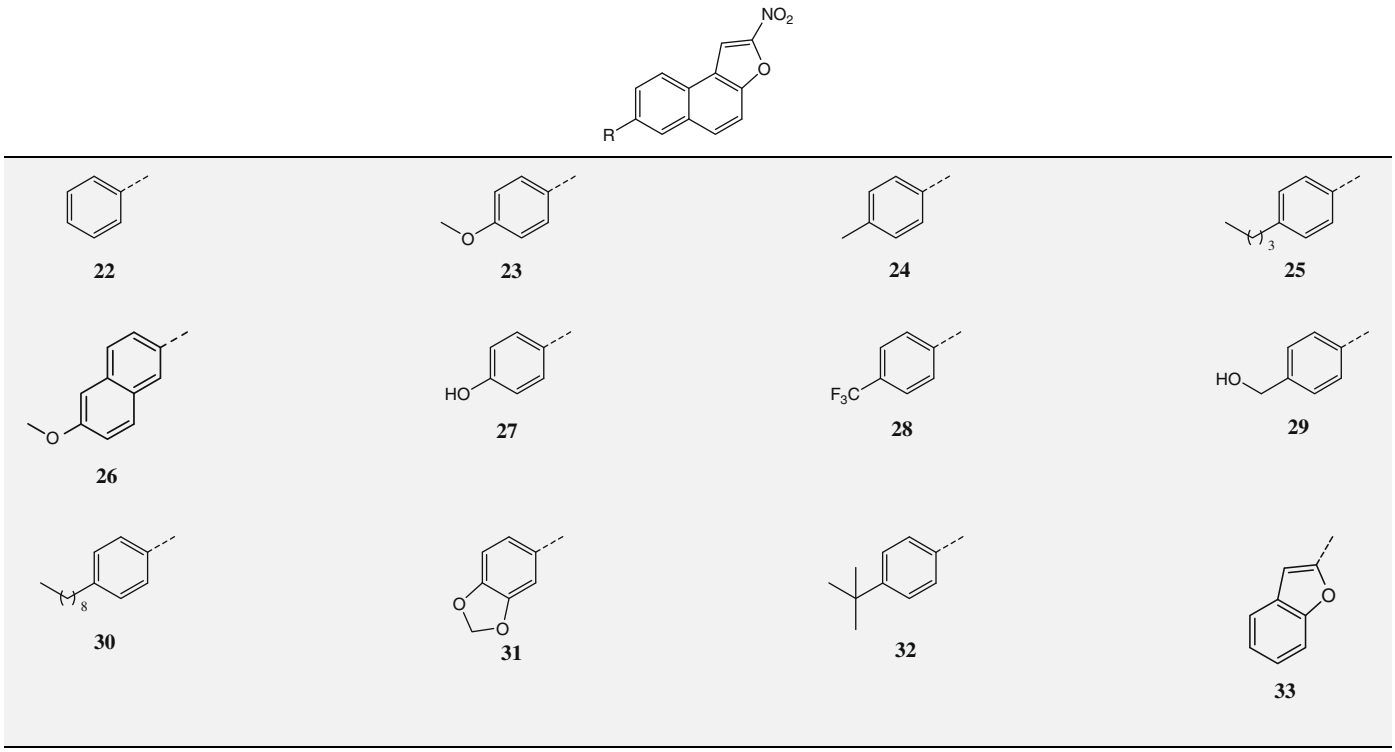

previous method. All the compounds **(7–17)** are described in Table 2. Excepted compounds **14** and **15**, all these synthesis have been adapted from synthesis previously reported by Royer et al.[18–20]

Compound **13** was converted into compound **14** by treatment with thionyl chloride then ammonia (73% yield). The beginning of the synthesis of compound **15** was adapted from synthesis of compound **9**. Then it was converted into ethyl 7-(2-ethoxy-2-oxo-ethoxy)naphtho[2,1-*b*]furan-2-carboxylate following a procedure used for compound **13**. Compound **15** was obtained by treatment with sodium hydroxide in a quantitative yield.

To complete the series, synthetic routes to 2-nitronaphtho[2,3-*b*]furan (**18**, Table 3), which have also been described by Royer,[21] were undertaken. Synthetic routes to (*E*)-6-methoxy-1-(2-nitrovinyl)naphthalen-2-ol (**19**) and 6-methoxy-1-(2-nitroethyl)naphthalen-2-ol (**20**, Table 3) have been adapted from a previously reported method for synthesis of 2-(2-nitroethyl)-phenols.[21]

Finally, we decided to introduce an aromatic ring in position 7 to increase the hydrophobicity of the ligands using 7-bromo-2-nitronaphthofuran (**21a**) as starting compound (Scheme 2).

Synthesis of this compound has been described by Royer and Buisson.[22] First, 6-bromo-2-naphthol (**21c**) was formylated in position 1 using tetrachloride titanium and dichloromethyl methyl ether. Second step is the condensation of bromonitromethane on **21b** to give 7-bromonitronaphthofuran (**21a**). Having secured a route to multigram quantities of the required intermediate, 7-bromo-2-nitronaphthofuran, attention was turned out to the investigation of the Suzuki–Miyaura coupling reaction.[14] Employing classical conditions, ($Pd(PPh_3)_4$, Na_2CO_3, toluene, ethanol, water), the palladium-catalyzed cross-coupling reaction of 7-bromo-2-nitronaphthofuran with a number of arylboronic acids was found to proceed smoothly in the presence of a base to give the corresponding biaryls in high yields (72–89%) (Table 4). Both electron rich (**31**) and electron-poor boronic acids (**28**) were found to couple in high yields. Indeed, these reactions were carried out with commercial grade boronic acid, using palladium complex as received.

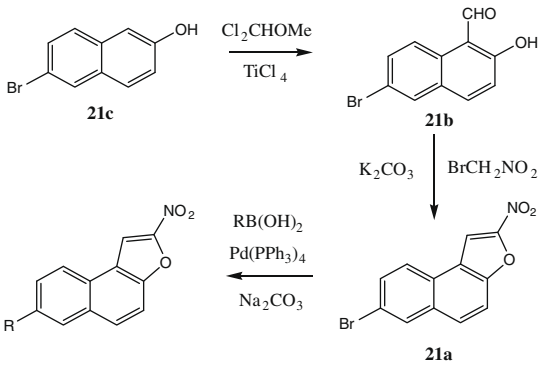

Scheme 2.

3. Results and discussion

3.1. Hit discovery

HNF4α agonist activities were evaluated using a one-hybrid system designed to express the full-length human nuclear receptor HNF4α fused in C-terminal of the DNA binding domain of the bacterial LexA protein in a yeast strain containing a β-galactosidase reporter gene controlled by a promoter harboring LexA binding sites. Screening of the National Center Institute (NCI, USA) diversity set of synthetic compounds with this system allowed us to discover that 4-methoxy-2-nitronaphtho[2,1-*b*]furan (compound **1**, see Fig. 1) enhances HNF4α-mediated transcriptional of the reporter gene activity with an EC_{50} close to 1.5 μM.

Such an activation was not observed when using other fusion proteins including either HNF4α-related proteins such as COUP-TFII or the estrogen receptor α (ERα), or the transcription activation domain of the unrelated yeast protein Gal4 (Fig. 1). Related molecules were found by screening the complete NCI library (250,000 compounds)

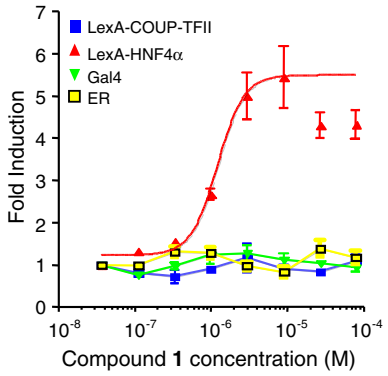

Figure 1. 4-Methoxy-2-nitro-naphtho[2,1-*b*]furan selectively activates HNF4α in yeast. Dose–response curves obtained with 4-methoxy-2-nitro-naphtho[2,1-*b*]furan in various yeast transformants. Increasing concentrations of compound were applied to yeast for 16 h before β-galactosidase assay. Note that β-galactosidase activity was enhanced only in HNF4α expressing cells in response to the compound.

with Chemfinder software (Cambridgesoft) by similarity search using 2-nitrobenzo[2,1-*b*]furan as a motif. Five new compounds were extracted to generate a first focused library (Table 1) and tested for their ability to regulate HNF4α in the yeast one-hybrid system. All the compounds were able to activate HNF4α-mediated transcription, although to different extents (Table 5). The compound leading to the highest β-galactosidase activity was found to be 7-methoxy-2-nitronaphtho[2,1-*b*]furan (**2**).

Initial screen was run with the full-length HNF4α fused to the LexA DNA binding domain and thus active compounds may modulate HNF4α via interactions outside the ligand binding domain. In order to delineate the domains required for the action of naphthofurans, we generated additional fusion proteins bearing various deletions (Fig. 2A).

Nuclear receptors usually possess two transcription activation domains called AF-1 and AF-2.[10] AF-1 is located in the N-terminal part of the protein, whereas AF-2 is generated by the folding of the ligand binding domain. HNF4α can be synthesized in vivo from alternative promoters generating two isoforms, HNF4α1 and HNF4α7, which differ in their N-terminal domains: whereas HNF4α1 harbors an AF-1 domain, HNF4α7 does not.[23–25] When using HNF4α7 in yeast one-hybrid assays, we found that compound **2** was still active, although the intrinsic transcriptional activity of the protein was low due to the lack of AF-1 (Fig. 2). When using the ligand binding domain only, deleted from the F domain and fused to the LexA DNA binding domain, the nitronaphthofuran still activated transcription, indicating that its activity is likely to rely on an interaction with the ligand binding domain of the receptor (Fig. 2). Since the F domain, a C-terminal extension of the protein beyond the ligand binding domain, has been shown to inhibit the transcriptional activity of AF-2 in HNF4α through an intramolecular folding mechanism inhibiting interaction with transcriptional coactivators,[24,25] our data suggest that compound **2** acts independently of this autoinhibitory process. Altogether, these data indicate that nitronaphthofurans may stabilize the active conformation of the nuclear receptor ligand binding domain, likely through a direct binding into the hydrophobic pocket.

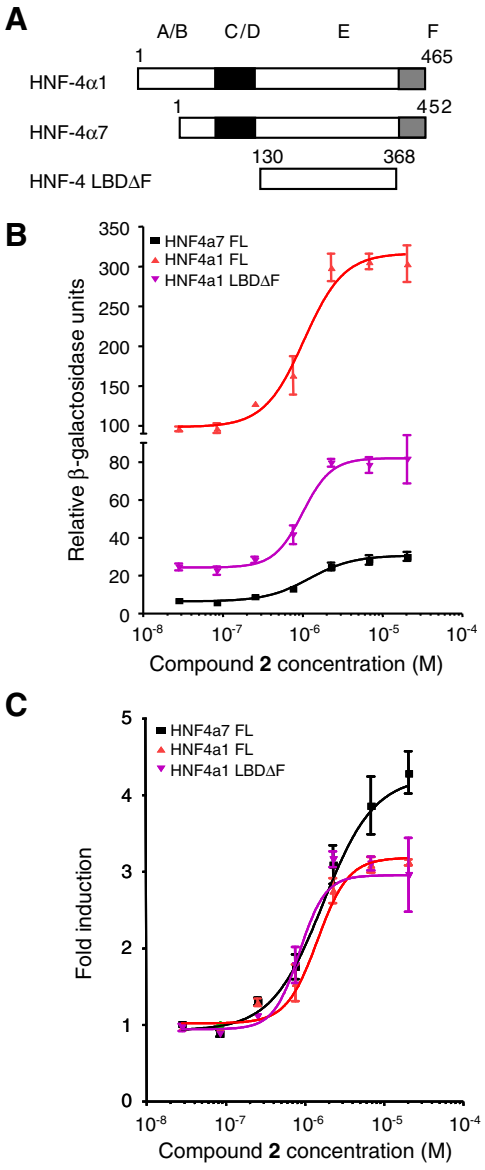

Figure 2. Compound **2** activates HNF4α through the ligand binding domain. (A) Schematic representation of HNF4α constructs used in this study. Numbers indicate amino-acids. Letters indicate the various functional domains of the protein with A/B: N-terminal domain harboring the transcription activation function 1 (AF-1), C/D: DNA binding and hinge domains, E: ligand binding domain, F: C-terminal domain. HNF4α1 and HNFα7 are naturally occurring variants generated by the use of two alternative promoters. (B and C) Activation of the different constructs in yeast one-hybrid assay by compound **2**. Increasing concentrations of compound were applied to yeast for 16 h before β-galactosidase assay. Note that deletion of AF-1 in HNF4α7 and the LBDΔF leads to a strong reduction in β-galactosidase activity (**B**) whereas the constructs are activated to a similar extent by compound **2** (**C**).

Table 5
EC_{50}s and IC_{50}s of selected compounds in yeast one-hybrid and MTT assays

	Compound	**1**	**2**	**3**	**4**	**5**	**6**	**7**	**14**
Yeast one hybrid	EC_{50} μM	1.47	2.57	2.09	2.33	1.28	1.22	1.95	>100
	Fold induction[a]	6.60	8.05	4.46	7.97	5.51	4.58	11.06	2
	@ (μM)	9.3	9.3	12.5	9.3	18.7	12.5	6.2	100
MTT assay	IC_{50}[b]	4.41	2.24	2.51	2.28	>5	2.04	5	>5

[a] Mean of fold induction in two independent experiments compared to DMSO.
[b] Mean of IC_{50} from two independent experiments.

3.2. Hit derivation

We then designed and synthesized a series of new compounds derived from the hit molecule 7-methoxy-2-nitronaphtho[2,1-*b*]furan, according to Scheme 1, and tested them in yeast one-hybrid assay. We essentially targeted the two opposite sides of the hit compound for modifications, namely carbon 2 and carbon 7 of the naphthofuran core. When leaving R_1 intact (i.e., NO_2), modification of R_2 led to inactive compounds except for compound **7** which showed a twofold increase in HNF4α activation when compared to the hit compound. The nitro group was then replaced by a carboxy group in order to phenocopy fatty acids. Nonetheless, compounds **12**, **13**, and **15** were all inactive. The requirement for the nitro group for high activity of the compounds was further confirmed through **10**, **11**, **14**, **16**, and **17** which were also mostly inactive, although compound **14** was able to activate twofold HNF4α at very high concentrations (Table 5). Finally, when large hydrophobic groups were added in R_2, activation of HNF4α was systematically lost (compounds **22–33**). Naphthol derivatives (compounds **19** and **21**) were also inactive. Hence, optimization of the hit compound generated a strong activator of HNF4α (compound **7**). However, a number of hit-derived compounds lost activity, especially in the absence of a nitro group, suggesting that the minimal backbone for an HNF4α activator is the nitronaphthofuran.

3.3. Coumpound 7 directly interacts with the HNF4α ligand binding domain

Since nitronaphthofurans activate HNF4 through the ligand binding domain, we examined binding of active compound **7** to HNF4α LBD by running two kinds of NMR experiments, namely Saturation Transfer Difference (STD) NMR and WaterLOGSY (Water–Ligand Observation with Gradient SpectroscopY).[26–31] Both techniques are known to be efficient methods to study protein–ligand recognition events and are classically used for drug screening. Both of them do not require any labeling or immobilization of either the ligand or the receptor and can be run using μM concentration range in protein and excess of ligand(s).

The choice of compound **7** among the active compounds was motivated by the criterion of complete solubility of this ligand in a minimal volume of deuterated organic solvent (10% DMSO-d_6) in order to preserve protein folding. Whereas compounds **1**–**5** were not soluble in 20 mM phosphate buffer pH 7.4, 100 mM NaCl containing 10% DMSO-d_6, compound **7** showed a total solubility from 30 up to 500 μM. The substitution in position 7 of the 2-nitronaphtho[2,1-*b*]furan by a polar group such as hydroxyl explains this higher solubility in water. In addition, according to the results of yeast one-hybrid assays, compound **7** is proposed to be a good candidate as a ligand. The apo-ligand binding domain of HNF4α was prepared from *E. coli* through a purification/renaturation protocol and therefore was devoid of fatty acids. As shown in Figure 3, STD and WaterLOGSY experiments gave identical results and suggested that compound **7** is an exchangeable ligand of HNF4α. Indeed, in STD experiments, signal from free ligand can only be observed if there is direct interaction within the protein binding site and dissociation of the bound ligand. In WaterLOGSY experiments, the negative sign of the free ligand signals is relevant of compound **7** binding to HNF4α. Hence, compound **7** unambiguously interacts with the ligand binding domain of HNF4α in vitro.

3.4. Coumpound 7 induces conformational changes in HNF4α ligand binding domain

The fluorescence-based thermal stability assay is used to identify ligands that stabilize a protein against thermal denaturation. This method measures fluorescence from a hydrophobic fluoroprobe

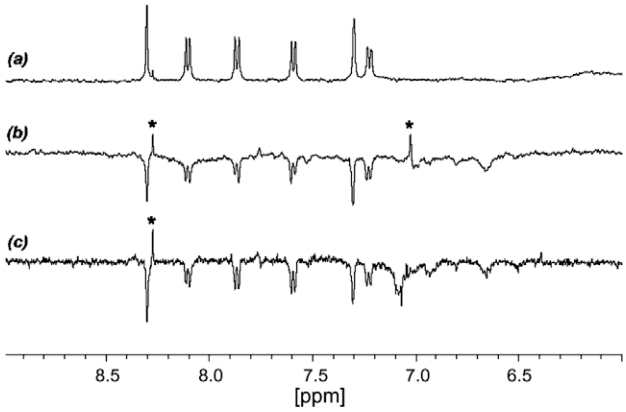

Figure 3. (a) Expanded region of one-dimensional reference spectrum recorded at 303 K for compound **7** (200 μM) in 20 mM phosphate buffer pH 7.4, 100 mM NaCl, 10% DMSO-d_6. Expanded region of (b) STD and (c) WaterLOGSY with NOE-ePHOGSY spectra recorded for compound **7** in the same conditions in presence of 30 μM HNF4α. Negative and positive signals in spectra (b) and (c) identify HNF4α interacting and not interacting molecules, respectively. The positive narrow peaks (*) originated from non-interacting molecules of the buffer.

whose emission properties change upon interaction with unfolded protein. The use of environmentally sensitive dyes to monitor thermal unfolding was reported in 1997[32] and later, this method was developed for drug discovery to allow rapid identification of ligands of target proteins from compound libraries.[33] The plot of fluorescence intensity versus temperature has a hyperbolic shape for a two-state unfolding mechanism and the melting temperature (T_m) is defined as the midpoint of temperature of the protein-unfolding transition. Very interestingly, thermofluor assay has been recently used to screen the ligand binding domain of another orphan nuclear receptor, estrogen-related receptor, and several classes of compounds that stabilized the receptor were identified.[34]

Purified apo-HNF4α LBD was subjected to gradually increasing temperature and the T_m values measured in the presence of the coactivator and/or potential ligand were compared with the T_m values for the control protein sample without any coactivator/ligand. Subsequently, the change in unfolding temperature, ΔT_m, was calculated. As seen from Figure 4, the addition of SRC-1 coactivator peptide slightly increased the T_m of the HNF4α LBD. Even though the co-crystal structure of HNF4α LBD and SRC-1 peptide has been published,[8] it seems that PGC-1 is the physiologically relevant HNF4α coactivator.[35] The thermal shift in the presence of PGC-1 peptide was indeed higher (0.84 ± 0.28 °C) and comparable with the one induced by compound **7** (1.06 ± 0.48 °C). Interestingly, the presence of both compound **7** and PGC-1 gave the highest average ΔT_m (1.43 ± 0.39) (Fig. 4), suggesting cooperative binding of both ligand and the coactivator peptide. These positive ΔT_m can be coupled to an increase in structural order and a reduced conformational flexibility. Most interestingly, the active compound **7** was able to stabilize the protein whereas thermal stability was unchanged in the presence of the natural ligand linoleic acid, which is inactive in mammalian cells,[12] as well as in our yeast one-hybrid system (data not shown).

3.5. Modeling compound interactions with the HNF4α ligand binding pocket

The ligand binding pocket of HNF4α has been described.[11] It is largely hydrophic in nature with only three polar residues (Ser181, Ser256 and Arg226). The charged residue (Arg226) is involved in a salt bridge with the carboxy group of fatty acids. We run docking experiments with compounds **1**, **2**, **5**, and **7** and the crystallized HNF4α ligand binding domain in the 'closed' conformation, after

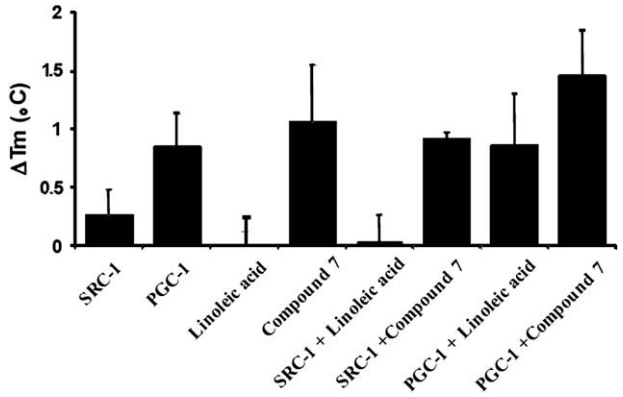

Figure 4. Thermal shift assay results for renatured HNF4α LBD in combination with its coactivators and potential ligands. The HNF4α LBD was aliquoted into wells of a 96-well plate at 0.4 mg/mL in the presence of SYPRO orange. Peptides and/or potential ligands were added in 3x molar excess and the plate was heated from 20 °C to 90 °C. Changes in the unfolding transition temperature (ΔT_m) are means from three to six independent experiments. Error bars represent the standard errors to the means.

protein minimization. As depicted in Figure 5, data suggested that all compounds could fit in the hydrophobic pocket of the nuclear receptor while generating few close contacts, especially with Ala223 and Leu236 (minimal distance between two atoms: 1.806 Å). Whereas compounds **2**, **5**, and **7** were predicted to generate bonds and hydrophobic interactions with the protein, compound **1** could only be engaged in hydrophobic interactions due to its quite different structure and position in the ligand binding pocket (additional Fig. S1). Interestingly, the most active compound (compound **7**) was predicted to generate two bonds with Arg226 and one bond with Ser256, whereas compounds **2** and **5** could form respectively one or two bonds with Arg226. Binding of a nitro group to an arginine residue (Arg288) has already been described for the ligand binding pocket of the nuclear receptor PPARγ occupied by nitrated linoleic acid.[36] Interestingly, despite being on two different helices, PPARγ Arg288 and HNF4α Arg226 positions are close in the ligand binding pocket (see additional Fig. S2). Since nitrated linoleic acid is a much stronger activator than linoleic acid,[37] it is possible that binding of nitro group at this position leads to productive conformational changes and could be viewed as a determinant of transcriptional activity. However, in view of the high activity of compound **1** in yeast-based assay, it is likely that hydrophobic interactions are crucial for binding to the protein and to achieve the structural rearrangements required for transcriptional activation. Alternatively, nitronaphthofurans may bind to another cryptic site to regulate the transcriptional activity of HNF4α.

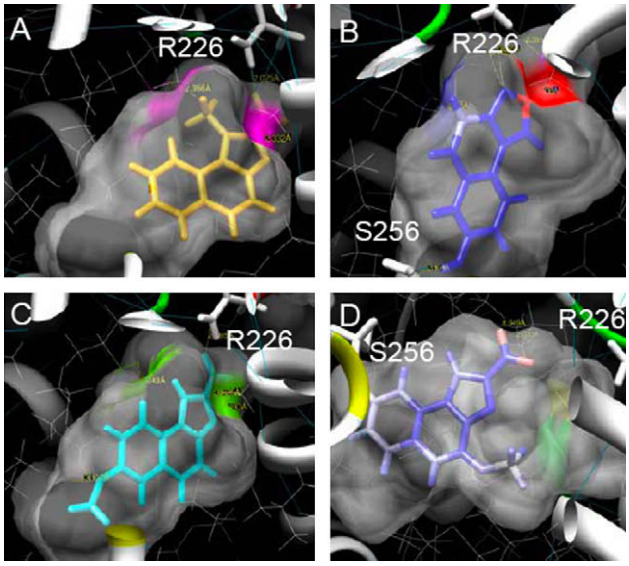

Figure 5. Modeling of compound **1**, **2**, **5**, and **7** in the ligand binding pocket of HNF4α. (A) Model of compound **5** bound in the ligand binding pocket of HNF4α (PDB 1m7w) generated by the docking software Gold 3.0. Images where generated with Chimera software. Polar residues have been highlighted in white (Arg226 and Ser256). The ligand binding pocket is shown as a grey cloud by 'surface' representation (50% transparency). (B) Model of compound **7** bound in the ligand binding pocket of HNF4α. (C) Model of compound **2** in the ligand binding pocket of HNF4α. (D) Model of compound **1** in the ligand binding pocket of HNF4α. Note that the presence of a methoxy group at position 4 shifts the nitro group away from Arg226. For A, B and C, color patches indicate close contacts with Leu236 and Ala223.

3.6. Modulation of HNF4α transcriptional activity in mammalian cells

Results obtained in yeast suggested that nitronaphthofurans presented either growth inhibiting or toxic effects on cells. Hence, we first undertook toxicity assays in human HepG2C3A hepatoma cells. Cells were treated with increasing concentrations of selected compounds during 24 h before being subjected to the classical MTT procedure. At the tested concentrations, all compounds were found to be highly toxic to human cells, except compound **5**, whose IC_{50} could not be determined within the range of concentrations tested (Table 5). Accordingly, only this compound was used for subsequent analysis of nitronaphthofuran impact on the transcriptional activity of HNF4α in cancer cells. Two known HNF4α responsive promoters (*ApoB* and *ApoCIII*) linked to the luciferase reporter gene were transfected, together with a HNF4α expression vector, in HepG2C3A cells which were then treated with compound **5** as well as with linoleic acid for 24 h. Expression of HNF4α strongly activated both reporter genes and linoleic acid showed no effect, as described earlier in similar reporter assays.[12] When compound **5** was added, both basal and HNF4α-induced transcriptional levels were partially reduced in a dose-dependent manner, but in different proportions. Accordingly, the ability of HNF4α to activate the reporter genes, as expressed in 'fold induction', increased with increasing concentrations of compound **5** (Fig. 6). This enhancement of HNF4α-driven activity was more pronounced with the *ApoCIII* reporter than with *ApoB* (Fig. 6A). At high concentrations, linoleic acid was also found to reduce both basal and HNF4α-induced activity of the reporter genes, but this did not result in any variation in the fold induction, except for the highest concentration, which led to a significant reduction in the level of HNF4α-driven transcriptional activity (Fig. 6B). Consistent with data obtained in yeast, these results indicate that compound **5**, despite a certain toxicity, is able to modulate HNF4α activity in human cells.

4. Conclusion

Screening of a chemical compound library led to the discovery of a family of small molecules activating the nuclear receptor HNF4α in a yeast cell-based assay. We further demonstrated that these compounds can bind directly to the ligand binding domain of the nuclear receptor, most likely in the hydrophobic pocket known to be occupied in vivo by linoleic acid.[12] Whereas the natural ligand (i.e., linoleic acid) does not seem to be able to regulate HNF4α transactivation function (our data and those from[12]), nitronaphthofurans can enhance HNF4α-driven activity. Interestingly, replacement of the nitro group by a carboxy group mimicking fatty

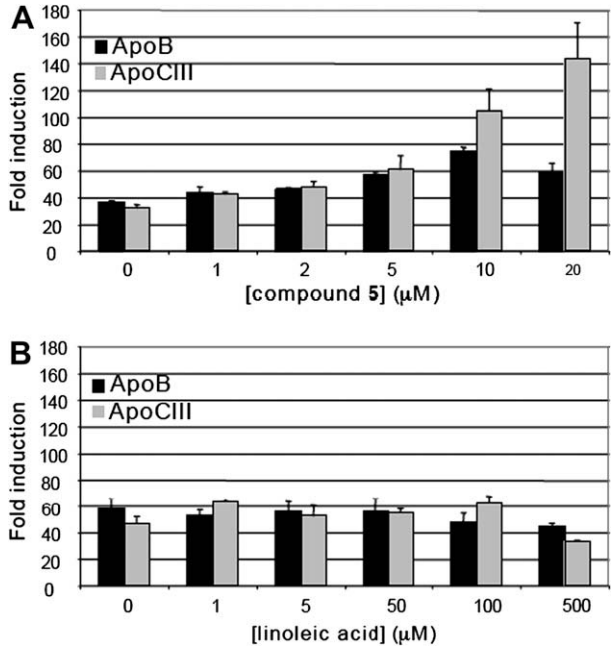

Figure 6. HNF4α transactivation function is regulated by compound **5** in cultured human cancer cells. HepG2C3A cells were transfected with *ApoB* and *ApoCIII* reporter genes together with a HNF4α expression vector. Cells were then treated for 24 h with compound **5** (A) or linoleic acid (B). Data are from one representative experiment run in triplicates and correspond to the ratio of HNF4α-induced versus basal luciferase expression levels (fold induction) for each concentration of ligand.

acids led to transcriptionally inactive compounds although they may bind to HNF4α (our NMR data, not shown). Hence, natural or synthetic ligand anchoring by a carboxy group is probably unable to induce conformational transitions which lead to a transcriptionally active structure. Further investigations of the nitro-specific structural remodeling of HNF4α ligand binding domain will certainly shed light on the structural determinants required for transcription activation by this particular nuclear receptor.

5. Experimental

5.1. Chemical synthesis

5.1.1. General remarks

All reactions were performed under argon. Solvents were distilled from appropriate drying agent prior to use: Et_2O and THF from sodium and benzophenone, toluene from sodium, CH_2Cl_2 from CaH_2, $CHCl_3$ from P_2O_5 and all other solvents were HPLC grade. Commercially available reagents were used without further purification unless otherwise stated. All reactions were monitored by TLC with Merck pre-coated aluminum foil sheets (Silica Gel 60 with fluorescent indicator UV_{254}). Compounds were visualized with UV light at 254 nm and 365 nm. Column chromatography was carried out using silica gel from Merck (0.063–0.200 mm). ^{1}H NMR was recorded using Bruker (Advance 300dpx and 200dpx spectrometers) at 300 MHz or 200 MHz. High-resolution mass spectra were recorded on a Varian MAT 311 Micromass spectrometer in EI mode at the CRMPO (Centre Régional de Mesures Physiques de l'Ouest, University of Rennes).

All the syntheses of the compounds belonging to the first series were adapted from a method previously reported excepted synthesis of compounds **14** and **15** and compounds resulting from Suzuki–Miyaura cross-coupling **(22–33)** which are described below.

5.1.1.1. Procedure for compound 14. To 157 mg of **12** (0.74 mmol) under argon and at 0 °C was added 81 μL (1.11 mmol) of thionyl chloride. The mixture was heated under reflux (65 °C) for 20 min. After cooling, the mixture was dried under vacuum to give a solid which was washed two times with 5 mL of dichloromethane. This solid was dissolved in 10 mL of THF at 0 °C and 10 mL of aqueous ammonia are slowly added. The mixture was stirred for 100 min at 0 °C then dried under vacuum. The residue was washed in 15 mL of water, filtered and the solid was washed two times with 10 mL of water to give 125 mg of a brown solid (73%); mp 186 °C, ^{1}H NMR: (200 MHz, $CDCl_3$), δ (ppm): 5.94 (sl, 1H, CO*NH*$_2$); 6.59 (sl, 1H, CO*NH*$_2$); 7.48–7.78 (m, 3H, 3ArH); 7.81–8.09 (m, 3H, 3ArH); 8.19 (d, 1H, J = 8.1 Hz) MS: $M^{+\cdot}$ calcd for $C_{13}H_9O_2$, 211.0633. Found: 211.0623.

5.1.1.2. Compound 15. Mp 212 °C, ^{1}H NMR: (300 MHz, DMSO-d_6), δ (ppm): 4.82 (s, 2H, O*CH*$_2$); 7.36 (d, 1H, J = 8.85 Hz, ArH); 7.50 (s, 1H, ArH); 7.75–7.95 (m, 2H, 2ArH); 8.30 (s, 1H, ArH); 8.36 (d, 1H, J = 8.90 Hz, ArH) MS: $M^{+\cdot}$ calcd for $C_{14}H_9NO_6$, 286.04774. Found: 286.0485.

5.1.2. General procedure used for Suzuki–Miyaura cross-coupling (22–33)

5.1.2.1. 7-(4-Methylphenyl)-2-nitronaphtho[2,1-b]furan (24). To a solution of 150 mg of **21a** (0.51 mmol) in 20 mL of a mixture (50/50) in toluene and ethanol under argon was added 105 mg (0.77 mmol) of 4-methoxybenzeneboronic acid, 82 mg (0.77 mmol) of sodium carbonate in 1.5 mL of water and 30 mg (0.03 mmol) of tetrakistriphenylphosphine palladium. The mixture was heated under reflux (90 °C) for 2 h. After cooling, the mixture was dried under vacuum to give a solid. The residue was also washed with water (30 mL), extracted three times with dichloromethane (30 mL) and the combined organic extracts were dried on sulfate magnesium. Dichloromethane was removed and the residue was purified by silica gel column chromatography and eluted with dichloromethane to give 118 mg (76%) of a yellow solid, mp 226 °C, ^{1}H NMR: (300 MHz, $CDCl_3$) δ 2.46 (s, 3H, Me); 7.35 (d, 2H, J = 7.93 Hz, 2ArH); 7.65 (d, 2H, J = 8.08 Hz, 2ArH); 7.72 (d, 1H, J = 9.11 Hz, ArH); 7.95 (d, 1H, J = 8.44 Hz, ArH); 8.07 (d, 2H, J = 9.16 Hz, ArH); 8.18 (s, 2H, 2ArH); 8.25 (d, 1H, J = 8.51 Hz, ArH) MS: $M^{+\cdot}$ calcd for $C_{19}H_{13}NO_3$, 303.0895. Found: 303.0890.

5.1.2.2. 2-Nitro-7-phenylnaphtho[2,1-b]furan (22). Yellow solid (80%), mp 206 °C, ^{1}H NMR: (500 MHz, $CDCl_3$) δ 7.45 (t, 1H, J = 7.53 Hz, ArH); 7.55 (t, 2H, J = 7.53 Hz, 2ArH); 7.77 (m, 3H, 3ArH); 8.00 (d, 2H, J = 6.71 Hz, ArH); 8.11 (d, 2H, J = 9.13 Hz, ArH); 8.22 (m, 2H, 2ArH); 8.27 (d, 1H, J = 8.51 Hz, ArH) MS: $M^{+\cdot}$ calcd for $C_{18}H_{11}NO_3$, 289.0739. Found: 289.0770.

5.1.2.3. 7-(4-Methoxyphenyl)-2-nitronaphtho[2,1-b]furan (23). Yellow solid (74%), mp 214 °C, ^{1}H NMR: (200 MHz, $CDCl_3$), δ 3.91 (s, 3H, OMe); 7.07 (d, 2H, J = 8.7 Hz, 2ArH); 7.71 (m, 3H, 3ArH); 7.90–8.30 (m, 5H, 5ArH) MS: $M^{+\cdot}$ calcd for $C_{19}H_{13}NO_4$, 319.0845. Found: 319.0838.

5.1.2.4. 7-(4-Butylphenyl)-2-nitronaphtho[2,1-b]furan (25). Yellow solid (88%), mp 152 °C, ^{1}H NMR: (300 MHz, $CDCl_3$), δ 0.98 (t, 3H, J = 7.32 Hz, CH_2CH_3); 1.43 (m, 2H, CH_2CH_3); 1.70 (m, 2H, $ArCH_2CH_2$); 2.71 (t, 2H, J = 7.55 Hz, $ArCH_2CH_2$); 7.35 (d, 2H, J = 8.07 Hz, 2ArH); 7.66 (d, 2H, J = 8.11 Hz, 2ArH); 7.72 (d, 1H, J = 9.14 Hz, ArH); 7.96 (d, 1H, J = 8.48 Hz, ArH); 8.07 (d, 2H, J = 9.17 Hz, ArH); 8.18 (s, 2H, 2ArH); 8.23 (d, 1H, J = 8.46 Hz, ArH) MS: $M^{+\cdot}$ calcd for $C_{22}H_{19}NO_3$, 345.1365. Found: 345.1366.

5.1.2.5. 7-(6-Methoxynaphthalen-2-yl)-2-nitronaphtho[2,1-b]furan (26). Orange solid (87%), mp 258 °C, ^{1}H NMR: (300 MHz, $CDCl_3$), δ 1.57 (s, 3H, OMe); 7.25–7.35 (m, 2H, 2ArH); 7.75 (d, 1H,

J = 9.14 Hz, ArH); 7.82–7.95 (m, 3H, 3ArH); 8.07–8.18 (m, 3H, 3ArH); 8.22 (s, 1H, ArH); 8.25–8.35 (m, 2H, 2ArH) MS: $M^{+\cdot}$ calcd for $C_{23}H_{15}NO_4$, 369.1001. Found: 369.0984.

5.1.2.6. 4-(2-Nitronaphtho[2,1-b]furan-7-yl)phenol (27). Red solid (72%), mp 251 °C, ^{1}H NMR: (300 MHz, DMSO-d_6), δ 6.92 (d, 2H, J = 8.53 Hz, 2ArH); 7.69 (d, 2H, J = 8.51 Hz, 2ArH); 7.95 (d, 1H, J = 9.14 Hz, ArH); 8.03 (d, 1H, J = 8.58 Hz, ArH); 8.24 (d, 1H, J = 9.20 Hz, ArH); 8.34 (s, 1H, ArH); 8.54 (d, 1H, J = 8.55 Hz, ArH); 8.91 (s, 1H, ArH); 9.65 (s, 1H, OH) MS: $M^{+\cdot}$ calcd for $C_{18}H_{11}NO_4$, 305.0688. Found: 305.0697.

5.1.2.7. 2-Nitro-7-(4-(trifluoromethyl)phenyl)naphtho[2,1-b] furan (28). Yellow solid (75%), mp 212 °C, ^{1}H NMR: (300 MHz, $CDCl_3$), δ 7.75–7.90 (m, 5H, 5ArH); 7.99 (d, 1H, J = 8.48 Hz, ArH); 8.12 (d, 1H, J = 9.14 Hz, ArH); 8.21 (s, 1H, ArH); 8.23 (s, 1H, ArH); 8.30 (d, 1H, J = 8.50 Hz, ArH) MS: $M^{+\cdot}$ calcd for $C_{19}H_{10}NO_3F_3$, 357.0613. Found: 357.0601.

5.1.2.8. (4-(2-Nitronaphtho[2,1-b]furan-7-yl)phenyl)methanol (29). Orange solid (84%), mp 247 °C, ^{1}H NMR: (300 MHz, DMSO-d_6), δ 4.58 (d, 2H, J = 5.44, CH_2OH); 5.27 (t, 1H, J = 5.60 Hz, CH_2OH), 7.47 (d, 2H, J = 8.09 Hz, 2ArH); 7.83 (d, 2H, J = 8.11 Hz, 2ArH); 7.98 (d, 1H, J = 9.18 Hz, ArH); 8.11 (d, 1H, J = 8.63 Hz, ArH); 8.30 (d, 1H, J = 9.23 Hz, ArH); 8.46 (s, 1H, ArH); 8.60 (d, 1H, J = 8.56 Hz, ArH); 8.95 (s, 1H, ArH) MS: $M^{+\cdot}$ calcd for $C_{19}H_{13}NO_4$, 319.0845. Found: 319.0869.

5.1.2.9. 2-Nitro-7-(4-nonylphenyl)naphtho[2,1-b]furan (30). Yellow solid (89%), mp 126 °C, ^{1}H NMR: (300 MHz, $CDCl_3$), δ 0.91 (t, 3H, J = 6.06 Hz, CH_2CH_3); 1.20–1.45 (m, 12H, $6CH_2$); 1.70 (m, 2H, $ArCH_2CH_2$); 2.70 (t, 2H, J = 7.54 Hz, $ArCH_2CH_2$); 7.35 (d, 2H, J = 8.03 Hz, 2ArH); 7.66 (d, 2H, J = 8.05 Hz, 2ArH); 7.73 (d, 1H, J = 9.15 Hz, ArH); 7.98 (d, 1H, J = 8.49 Hz, ArH); 8.08 (d, 2H, J = 9.17 Hz, ArH); 8.19 (s, 2H, 2ArH); 8.24 (d, 1H, J = 8.48 Hz, ArH) MS: $[M-CH_3]^+$ calcd for $C_{26}H_{26}NO_3$, 400.1913. Found: 400.1902.

5.1.2.10. 7-(Benzo[d][1,3]dioxol-5-yl)-2-nitronaphtho[2,1-b] furan (31). Orange solid (88%), mp 280 °C, ^{1}H NMR: (300 MHz, DMSO-d_6), δ 5.76 (s, 2H, OCH_2O); 7.07 (d, 1H, J = 8.07 Hz, ArH); 7.36 (d, 1H, J = 8.14 Hz, ArH); 7.47 (s, 1H, ArH); 7.98 (d, 1H, J = 9.15 Hz, ArH); 8.06 (d, 1H, J = 8.62 Hz, ArH); 8.26 (d, 1H, J = 9.16 Hz, ArH); 8.40 (s, 1H, ArH); 8.57 (d, 1H, J = 8.56 Hz, ArH); 8.94 (s, 1H, ArH) MS: $M^{+\cdot}$ calcd for $C_{19}H_{11}NO_5$, 333.0637. Found: 333.0611.

5.1.2.11. 7-(4-tert-Butylphenyl)-2-nitronaphtho[2,1-b]furan (32). Yellow solid (86%), mp 202 °C, ^{1}H NMR: (300 MHz, $CDCl_3$), δ 1.42 (s, 9H, Me); 7.56 (d, 2H, J = 8.37 Hz, 2ArH); 7.65–7.75 (m, 3H, 3ArH); 8.00 (d, 1H, J = 8.46 Hz, ArH); 8.09 (d, 2H, J = 9.16 Hz, ArH); 8.19 (s, 2H, 2ArH); 8.25 (d, 1H, J = 8.46 Hz, ArH) MS: $M^{+\cdot}$ calcd for $C_{22}H_{19}NO_3$, 345.1365. Found: 345.1331.

5.1.2.12. 7-(Benzofuran-2-yl)-2-nitronaphtho[2,1-b]furan (33). Orange solid (88%), mp 266 °C, ^{1}H NMR: (300 MHz, DMSO-d_6), δ 7.25–7.40 (m, 2H, 2ArH); 7.65–7.75 (m, 3H, 3ArH); 8.03 (d, 1H, J = 9.14 Hz, ArH); 8.30–8.40 (m, 2H, 2ArH); 8.59–8.72 (m, 2H, 2ArH); 8.96 (s, 1H, ArH) MS: $M^{+\cdot}$ calcd for $C_{20}H_{11}NO_4$, 329.0688. Found: 329.0663.

5.2. Biology

5.2.1. Materials and cloning

All yeast media were from Sigma–Aldrich. The synthetic compound library as well as individual compounds from Table 1 were obtained from the National Cancer Institute (USA). For screening of compound activity we used the DupLex-A™ yeast two-hybrid system from OriGene Technologies, Inc. (Rockville MD, USA). The HNF4α1 expression vector as well as the cDNA for human and rat HNF4α were gifts from Dr Talianidis (Athens). Full-length human HNF4α1 and human HNF4α7 were transferred in frame with the LexA DNA binding domain (DBD) in the one-hybrid vector pEG202 (OriGene Technologies, Inc.), after digestion with BamHI/NotI for HNF4α1 and EcoRI/NotI for HNF4α7. The rat HNF4α LBD (aa 130–368) cDNA was transfered in frame from pGEX-6P-1 (GE Healthcare) to pEG202 through EcoRI digestion. The human COUP-TFII cDNA encoding aa 52–414 was amplified by PCR (forward primer: 5′-ACGCCATGGCAGACGGC-3′, reverse primer: 5′-CTGTTTCACTCGAGCTTCTT ATTTTA-3′) and was inserted in frame with the LexA DBD in pEG202 after restriction digest with *Nco*I and *Xho*I. The YEphER and the control Gal4 yeast expression vectors were as previously described.[38] The *ApoCIII* and *ApoB*-Luciferase reporter plasmids were gifts from Dr. Sladek (Riverside, California) and have been described.[39,40]

5.2.2. One-hybrid assays and library screening

Compounds from the NCI library were tested in a 96-well-plate format assay as described,[41] using the LexADBD-HNF4α1 one-hybrid system. In this assay, the LexADBD-HNF4α1 fusion protein binds to the promoter of the β-galactosidase gene and activates transcription. Thus, the production of β-galactosidase in the cell reflects the transcriptional activity of the fusion protein. Compounds were given to cells in DMSO (1% highest final concentration). Control experiments run with DMSO alone were used to correct for the solvent effect. After cell lysis, β-galactosidase activity was revealed with the fluorescent substrate 4-Methylumbelliferyl β-D-galactopyranoside (4-MUG, Sigma–Aldrich) at a final concentration of 40 μg/mL. In the primary screen, each compound was assessed at three concentrations in triplicates (1.6×10^{-6} M, 8×10^{-6} M, and 4×10^{-5} M). Compounds that induced at least a twofold increase in HNF4α-mediated transcriptional activity were selected for a secondary screen with concentrations ranging from 4×10^{-8} M to 10^{-4} M. Only those compounds showing a robust and consistent activation of HNF4α were selected for further analysis. EC_{50}s were deduced from activation curves obtained in yeast one-hybrid assays.

5.2.3. Toxicity assay

One hundred microliters of HepG2C3A cells (ATCC, CRL-10741) at a concentration of 300 cells/μL were inoculated to each of the 96-well plate and cultured for 24 h. Confluent cells were treated with various concentrations of compounds from 0.002 μM to 5 μM to flank EC_{50} determined in yeast one-hybrid experiment, while DMSO (0.05%) was used as the negative control. Each condition was performed in quadruplicate. After treatment for another 48 h, 10 μL MTT (3-[4,5-dimethylthiazol-2-yl]-2,5-diphenyltetrazolium bromide; Thiazolyl blue, 5 mg/mL) were added to each well and cultured for 2 h. Then, after removing the medium, formazan crystals were dissolved in 100 μL DMS0. Absorbance was measured at 570 nm and background at 630 nm using microplate reader (Power Wave X5; Biotek). Data were acquired using KC4 version 3.4 software (Biotek instruments Inc.). Results (% of cell viability) were calculated as follows: $[(A_{570}-A_{630})$ compound$/(A_{570}-A_{630})$ DMSO]X100. Results were from two independent experiments.

5.2.4. Transfection assays

HepG2C3A cells were plated at a density of 6×10^4 per well in 24-wells plates in Dulbecco's Modified Eagle Medium (DMEM, Invitrogen), 24 h before transfection. Cells were transfected using JetPEI reagent (polyplus-transfection) according to manufacturer's instructions. Briefly, cells were transfected using 800 ng of total

plasmid DNA [250 ng of reporter plasmid (ApoB-Luc or ApoCIII-Luc), 250 ng of plasmid coding β-galactosidase (pCH-110), 50 ng of plasmid coding full-length HNF4α (HNF4α-pCR3.1) and plasmid pCR3.1 as ballast to complete to 800 ng] during 24 h in 500 μL of DMEM. Then, media were removed and cells were treated using increasing concentrations of compound **5** (from 1 μM to 20 μM), linoleic acid (from 1 μM to 500 μM) or DMSO 0.5% as control, during 24 h. At the end of treatment, media were removed and 100 μL of Reporter Lysis Buffer (Promega) were directly added into each well of plates which were frozen (−80 °C) during 24 h. Cells were then harvested, transferred into microtubes and centrifuged (14,000 rpm, 1 min, 4 °C). Supernatants were collected and 30 μL were used to quantify luciferase activity using Luciferase Assay System (Promega) following supplier's recommendations. To determine transfection efficiency, β-galactosidase activity was measured using 4-methylumbelliferyl β-D-galactopyranoside (4-MUG) fluorescent substrate (Sigma Aldrich). Briefly, 40 μL of 2X concentrated 4-MUG solution (80 μg/mL) were added to 40 μL of supernatant and fluorescence was read (excitation 365 nm, emission 450 nm) in a microplate-reading fluorimeter (Fluorolite 1000, Dynatech Laboratories). All experiments were performed at least three times in independent manner in triplicates and fold induction activities were calculated as follows: [(mean of luciferase activity)$_{[compound]}$/(mean of β-gal activity)$_{[compound]}$]/[(mean of luciferase activity)$_{DMSO}$/(mean of β-gal activity)$_{DMSO}$]. Standard deviations were calculated using triplicate values in each independent experiment.

5.3. NMR

5.3.1. NMR samples

Ligand stock solution of 10 mM was prepared in DMSO-d_6. 10 μL of this stock solution was diluted in 450 μL of 30 μM apo HNF4α LBD solution prepared in 20 mM phosphate buffer pH 7.4 containing 100 mM NaCl. 40 μL of DMSO-d_6 were added. The final ligand concentration was 200 μM. A reference tube containing only the ligand (without protein) was prepared with identical conditions.

5.3.2. Acquisition of NMR spectra

All NMR spectra were recorded at 303 K with a spectral width of 14 ppm on Bruker Avance 500 MHz spectrometer, equipped with a 5 mm TXI inverse triple-resonance cryoprobe head. (PRISM platform, University of Rennes 1, France).

5.3.3. STD (Saturation Transfer Difference) experiments

Selective saturation of the protein was achieved by a train of Gauss-shaped pulses of 50 ms length each, truncated at 1%, and separated by a 1 ms delay. 40 selective pulses were applied, leading to a total length of the saturation train of 2 s. The on-resonance irradiation of the protein was performed at a chemical shift of 0.7 ppm. Off-resonance irradiation was set at 40 ppm, where no protein signals are present. Unwanted magnetization water was suppressed using a WATERGATE 3-9-19 pulse sequence. A 30 ms spin lock pulse was applied to remove protein background signals. Total scan number in the STD experiments was 128. The spectra on- and off-resonance were subtracted after multiplication by an exponential line-broadening function of 0.5 Hz prior to Fourier transformation. Spectra processing was performed using TOPSPIN 1.3 software (Bruker).

5.3.4. WaterLOGSY (Water–Ligand Observation with Gradient SpectroscopY) experiments

The details of the pulse sequence version used for the WaterLOGSY experiment reported here, using ePHOGSY-NOE selective excitation with a 180 shaped pulse at H_2O position or at another frequency, can be found in the literature.[29–31] A reference 1D spectrum of the ligand alone and a 1D WaterLOGSY spectrum in the presence of the protein were recorded. The first water selective 180° pulse, which does not require high selectivity, was applied during 5 ms. The first two Pulsed Field Gradients (PFGs) had a typical duration of 2 ms. This strength is sufficient to destroy the unwanted magnetization and, at the same time, it avoids signal losses due to diffusion occurring between the first two PFGs. A weak rectangular PFG is applied during the entire length of the mixing time (1 s). A short gradient recovery time of 1 ms is applied at the end of the mixing time before the detection pulse. The water suppression in both experiments was achieved with the excitation sculpting sequence (Hwang and Shaka, 1995). The data were collected with a sweep width of 14 ppm, an acquisition time of 0.584 s, and a relaxation delay of 2 s. Prior to Fourier transformation the data were multiplied with an exponential function with a line-broadening of 0.5 Hz.

5.4. Thermofluor assays

Ligand binding domain of human HNF4α (amino-acids 133–368) has been cloned into expression vector pETM11 (EMBL, Heidelberg) containing 6xHis tag and proteolytic cleavage site for TEV protease. Recombinant protein was bacterially expressed and purified under denaturing conditions. Purification, renaturation and tag cleavage of HNF4α LBD will be published elsewhere (Dudasova et al., manuscript in preparation). In thermofluor assay, the coactivator peptides bearing the following primary sequence were used: SRC-1 (NH2-RHKILHRLLQEGSPS-COOH); PGC-1 (NH2-EEPSLLKKLLLAPANT-COOH).

A real-time PCR device (Roche) was used to monitor protein-unfolding by the increase in the fluorescence of the fluorophor SYPRO Orange (Sigma Aldrich S5692). Protein sample (final concentration of 0.3 mg/mL or 11 μM) in 20 mM Tris–Cl buffer (pH 8.0) containing 100 mM NaCl and the 3× molar excess of the test compound (33 μM final concentration) in a reaction volume of 20 μL were incubated in 96-well microplates covered by optical foil. Water was added instead of test compound in the control samples. SYPRO Orange was diluted 100× to yield a 20× working concentration. The thermofluor assay was performed using Light Cycler 480 Instrument II (Roche) by increasing the temperature at 1 °C/min ranging from 20 to 90 °C and data points were collected in 1 °C intervals. The wavelengths for excitation and emission were 498 and 580 nm, respectively. Melting temperatures for individual wells were established by analysis with provided software. In the absence of ligands (control), $T_m = T_0$, and the ligand-dependent changes in midpoint temperature, $\Delta T_m = T_m - T_0$, were calculated for individual samples.

5.5. Methods for computer-simulated ligand binding (docking)

5.5.1. Protein input file preparation

A clean HNF4α input file was generated by using the protein preparation wizard of Maestro software (Maestro 8.5, academic campaign, http://www.schrodinger.com). The protein was cleaned by removing water molecules, ligands and subunits b, c and d from the 1m7w original pdb file. The bond order was assigned and Hydrogen atoms were added. The cleaned protein was minimized using the CHARMm22 molecular mechanic force field implemented in Hyperchem 8.0 software (Hypercube, Inc.) using the Fletcher-Reeves conjugate gradient algorithm. The resulting receptor (HNF4α a subunit) was saved to a PDB file.

5.5.2. Ligand input file preparation

The ligand input structure was generated and 3d optimized with MarvinSketch Academic Package (MarvinSketch 5.1.4, 2008,

ChemAxon http://www.chemaxon.com). The ligand structure was saved as a mol2 file.

5.5.3. Gold 3.0 docking protocol

For the study, the binding pocket of the receptor was defined from the crystallographic coordinates of Met182. Dockings were performed under standard default settings of GOLD software (CCDC Software Ltd, Cambridge): population size of 100, number of islands of 5, number of operations 100,000, niche size of 2 and a selection pressure of 1.1. Images were generated with Chimera software (UCSF).

Acknowledgments

We thank the National Cancer Institute (USA) for providing compounds. We also thank Maud Bizot, Gaëlle Palierne and Catherine Martin for technical support. We are grateful to Dr. Eeckhoute for critical reading of the manuscript. This work was funded by the European Community (QLG1-CT-2001-01513 and LSHM-CT-2006-037498), the Région Bretagne (SIE 211-B3-11), the Centre National pour la Recherche Scientifique and the Ministère de l'enseignement supérieur et de la recherche.

Supplementary data

Supplementary data associated with this article can be found, in the online version, at doi:10.1016/j.bmc.2009.07.079.

References and notes

1. Akiyama, T. E.; Gonzales, F. J. *Biochim. Biophys. Acta* **2003**, *1619*, 223.
2. Bogan, A. A.; Dallas-Yang, Q.; Ruse, M. D., Jr.; Maeda, Y.; Jiang, G.; Nepomuceno, L.; Scanlan, T. S.; Cohen, F. E.; Sladek, F. M. *J. Mol. Biol.* **2000**, *302*, 831.
3. De Fabiani, E.; Mitro, N.; Anzulovich, A. C.; Pinelli, A.; Galli, G.; Crestani, M. *J. Biol. Chem.* **2001**, *276*, 30708.
4. Inoue, Y.; Yu, A. M.; Yim, S. H.; Ma, X.; Krausz, K. W.; Inoue, J.; Xiang, C. C.; Brownstein, M. J.; Eggerstein, G.; Björkhem, I.; Gonzales, F. J. *J. Lipid Res.* **2006**, *47*, 215.
5. De Fabiani, E.; Mitro, N.; Gilardi, F.; Caruso, D.; Galli, G.; Crestani, M. *J. Biol. Chem.* **2003**, *278*, 39124.
6. Hertz, R.; Magenheim, J.; Berman, I.; Bar-Tana, J. *Nature* **1998**, *392*, 512.
7. Bogan, A. A.; Dallas-Yang, Q.; Ruse, M. D., Jr; Maeda, Y.; Jiang, G.; Nepomuceno, L.; Scanlan, T. S.; Cohen, F. E.; Sladek, F. M. *J. Mol. Biol.* **2000**, *302*, 831.
8. Duda, K.; Chi, Y. I.; Shoelson, S. E. *J. Biol. Chem.* **2004**, *279*, 23311.
9. Wisely, G. B.; Miller, A. B.; Davis, R. G.; Thornquest, A. D., Jr.; Johnson, R.; Spitzer, T.; Sefler, A.; Shearer, B.; Moore, J. T.; Miller, A. B.; Wilson, T. M.; Williams, S. P. *Structure* **2002**, *10*, 1225.
10. Gronemeyer, H.; Gustafsson, J. A.; Laudet, V. *Nat. Rev. Drug Disc.* **2004**, *3*, 950.
11. Dhe-Paganon, S.; Duda, K.; Iwamoto, M.; Chi, Y. I.; Shoelson, S. E. *J. Biol. Chem.* **2002**, *277*, 37973.
12. Yuan, X.; Ta, T. C.; Lin, M.; Evans, J. R.; Dong, Y.; Bolotin, E.; Sherman, M. A.; Forman, B. M.; Sladek, F. M. *Plos One* **2009**, *4*, e5609.
13. Royer, R.; Buisson, J. P. *Eur. J. Med. Chem.* **1983**, *18*, 79.
14. Miyaura, M.; Suzuki, A. *Synth. Commun.* **1981**, *11*, 513.
15. Royer, R.; Demerseman, P.; René, L. *Bull. Soc. Chim. Fr.* **1970**, *10*, 3740.
16. Tromelin, A.; Demerseman, P.; Royer, R. *Synthesis* **1985**, 1074.
17. Einhorn, J.; Lamotte, G.; Buisson, J. P.; Demerseman, P.; Royer, R. *Eur. J. Med. Chem.* **1984**, *19*, 143.
18. Cavier, R.; Buisson, J. P.; Lemoine, J.; Royer, R. *Eur. J. Med. Chem.* **1981**, *16*, 73.
19. Royer, R.; Buisson, J. P.; Rene, L. *Bull. Soc. Chim. Fr.* **1972**, *11*, 4158.
20. Dixit, M.; Sharon, A.; Maulik, P. R.; Goel, A. *Synlett* **2006**, 1497.
21. Dauzonne, D.; Royer, R. *Synthesis* **1984**, 1054.
22. Royer, R.; Buisson, J. P. *Eur. J. Med. Chem.* **1980**, *15*, 275.
23. Thomas, H.; Jaschkowitz, K.; Bulman, M.; Frayling, T. M.; Mitchell, S. M.; Roosen, S.; Lingott-Frieg, A.; Tack, C. J.; Ellard, S.; Ryffel, G. U.; Hattersley, A. T. *Hum. Mol. Genet.* **2001**, *10*, 2089.
24. Eeckhoute, J.; Moerman, E.; Bouckenooghe, T.; Lukoviak, B.; Pattou, F.; Formstecher, P.; Kerr-Conte, J.; Vandewalle, B.; Laine, B. *Endocrinology* **2003**, *144*, 1686.
25. Ruse, M. D., Jr.; Privalsky, M. L.; Sladek, F. M. *Mol. Cell. Biol.* **2002**, *22*, 1626.
26. Mayer, M.; Meyer, B. *Angew. Chem., Int. Ed.* **1999**, *38*, 1784.
27. Piotto, M.; Saudek, V.; Sklenar, V. *J. Biomol. NMR* **1992**, *2*, 661.
28. Sklenar, V.; Piotto, M.; Leppik, R.; Saudek, V. *J. Magn. Reson., Ser A* **1993**, *102*, 241.
29. Dalvit, C. *J. Magn. Reson., Ser B* **1996**, *112*, 282.
30. Dalvit, C.; Ramage, P.; Homme, U. *J. Magn. Reson.* **1998**, *131*, 148.
31. Dalvit, C.; Pevarello, P.; Tato, M.; Veronesi, M.; Vulpetti, A.; Sundstrom, M. *J. Biomol. NMR* **2000**, *18*, 65.
32. Poklar, N.; Lah, J.; Salobir, M.; Macek, P.; Vesnaver, G. *Biochemistry* **1997**, *36*, 14345.
33. Pantoliano, M. W.; Petrella, E. C.; Kwasnoski, J. D.; Lobanov, V. S.; Myslik, J.; Graf, E.; Caryer, T.; Asel, E.; Springer, B. A.; Lane, P.; Salemme, F. R. *J. Biomol. Screen.* **2001**, *6*, 429.
34. Abad, M. C.; Askari, H.; O'Neill, J.; Klinger, A. L.; Milligan, C.; Lewandowski, F.; Springer, B.; Spurlino, J.; Rentzeperis, D. *J. Steroid Biochem. Mol. Biol.* **2008**, *108*, 44.
35. Yoon, J. C.; Puigserver, P.; Chen, G.; Donovan, J.; Wu, Z.; Rhee, J.; Adelmant, G.; Stafford, J.; Kahn, C. R.; Granner, D. K.; Newgard, C. B.; Spiegelman, B. M. *Nature* **2001**, *413*, 131.
36. Li, Y.; Zhang, J.; Schopfer, F. J.; Martynowski, D.; Garcia-Barro, M. T.; Kovach, A.; Suino-Powell, K.; Baker, P. R.; Freeman, B. A.; Chen, Y. E.; Xu, E. *Nat. Struct. Mol. Biol.* **2008**, *15*, 865.
37. Schopfer, F. J.; Lin, Y.; Baker, P. R.; Cui, T.; Garcia-Barro, M.; Zhang, J.; Chen, K.; Chen, Y. E.; Freeman, B. A. *Proc. Natl. Acad. Sci. U.S.A.* **2005**, *102*, 2340–2345.
38. Métivier, R.; Petit, F. G.; Valotaire, Y.; Pakdel, F. *Mol. Endocrinol.* **2000**, *14*, 1849.
39. Sladek, F. M.; Dallas-Yang, Q.; Nepomuceno, L. *Diabetes* **1998**, *47*, 985.
40. Dallas-Yang, Q.; Jiang, G.; Sladek, F. M. *BioTechniques* **1998**, *24*, 580.
41. Le Guével, R.; Pakdel, F. *Biotechniques* **2001**, *30*, 1000.